Automation in Construction 176 (2025) 106296

Contents lists available at ScienceDirect

Automation in Construction

journal homepage: www.elsevier.com/locate/autcon

Semi-autonomous aerial robot for ultrasonic assessment of crack depth and surface velocity in concrete structures

Luca Belsito [a], Diego Marini [a], Luca Masini [a], Matteo Ferri [a,*], Miguel Ángel Trujillo [b], Antidio Viguria [b], Alberto Roncaglia [a]

[a] Institute for Microelectronics and Microsystems (IMM), National Research Council of Italy (CNR), Italy
[b] Advanced Center for Aerospace Technologies (CATEC), Spain

ARTICLE INFO

Keywords:
UAV
Robotic arm
Ultrasound measurements
Autonomous inspection
Cracks
Concrete

ABSTRACT

The measurement of ultrasonic surface velocity in concrete and the ultrasonic Time Of Flight method for estimating the depth of surface opening cracks in concrete are important techniques for maintenance of constructions, which are currently performed manually. This paper demonstrates the possibility to automate these measurements by means of an Unmanned Aerial Vehicle (UAV) equipped with a robotic arm, avoiding the risks and costs related to the manual methods. The automated measurements are performed by a special end effector with closed-loop force control that maintains the flying UAV stable while the robotic arm contacts the concrete surface with two piezoelectric transducers for the ultrasonic tests. The system is successfully validated by performing ultrasound measurements from the flying UAV on a test specimen with artificial cracks and on the T9 Metsovo bridge in Greece during an on-field trial, demonstrating an error margin lower than 1 % on crack depth.

1. Introduction

Maintenance, inspection, and monitoring of bridges are expected to become prominent issues of Europe policymaking processes in the next years [1]. More than 1234 km of road bridges with height over 100 m are spread across Europe; if smaller bridges are included, the number is significantly higher. Considering that most of the transport bridge stock built after 1945 was expected to have a design life of 50–100 years and that most of those bridges are still operational today, these infrastructures must be carefully monitored in order to avoid disasters such as the Genova Bridge collapse in 2018 and ensure a safe and regular serviceability [2]. The EU-funded BRIME project estimated that highway bridges in three different European countries (France, Germany and the UK) present deficiencies at a rate of 39 %, 30 % and 37 % respectively, highlighting the urgent need for frequent and massive inspection of such structures [3].

The inspection operations that are routinely performed on bridges consist of visual detection of delamination, corrosion and surface opening cracks, measurement of crack widths and depths, rebar analysis and estimation of beam deflection. Measurements on surface opening cracks are commonly conducted manually by a human operator with measurement tools such as strings, graduated scales or crack comparators [4]. The main issues related to such operations stem from the manual methods employed in the measurements and from the difficulties and risks encountered by the operators in reaching the cracks. Regarding the first issue, low accuracy and traceability, subjectivity in reading and difficulties in data recording are commonly considered to impair the reliability of the work; this demands many repetitive measurements to achieve accurate values, increasing the workload of the operators. On the other hand, since these workers usually need to access the inspection areas of the structure using lifters, ladders and scaffoldings, such operations may lead to serious safety problems for the workers involved and inconveniences for road users, due to traffic interruption or limitation [5]. The time required for the measurements, the need to employ highly experienced workers and the related costs have been directing research towards automation-oriented alternatives [6–11].

The use of UAV platforms equipped with cameras and sensors as aerial stations for monitoring operations could provide the technological basis for a revolutionary way to inspect difficult-to-access areas on constructions. Computer vision systems integrated on UAVs that use digital image processing for automatic inspection of surface defects have already been demonstrated and are expected to overcome the drawbacks of traditional visual inspection [7–12]. Moreover, the evolution of UAV

* Corresponding author.
E-mail address: matteo.ferri@cnr.it (M. Ferri).

https://doi.org/10.1016/j.autcon.2025.106296
Received 10 January 2025; Received in revised form 19 May 2025; Accepted 19 May 2025
Available online 29 May 2025

technology has led to the possibility to integrate end-effectors able to manipulate objects with unprecedented accuracy and to even operate in contact with structures. In particular, aerial manipulators composed of an aerial platform and a robotic arm have already shown the ability to conduct inspection tasks that require contact and hovering stability [13]. In the field of structural assessment, UAV systems exploiting the aerial stability obtained through the ceiling effect have been presented, performing high precision estimations of bridge beam deflection in a relevant application environment [14]. Furthermore, research prototypes and commercial systems that can contact vertical, horizontal and inclined surfaces to perform ultrasonic wall thickness measurement through ultrasonic testing have been reported [15–17].

However, these systems still have limitations that make them unsuitable for use on concrete and, so far, only UAV-based ultrasound measurements on metallic materials such as steel have been presented. For the measurement of crack depth and width in concrete [18,19], it is fundamental to bring the ultrasonic transducers in contact with the surface of the structure near the surface opening of the crack, with a placement error in the order of few centimetres. This requirement is very challenging for the contacting techniques presented so far for ultrasonic measurements from UAVs, which are based on direct contact with the measurement surface while the vehicle is in hovering (steady flight) conditions. With these techniques, once contact is established, the UAV can maintain the position of the end-effector during the measurement but cannot adjust it in any way. Because of this limitation, the required placement accuracy of few centimetres is very difficult to reach, unless the contact procedure is repeated several times, which would make the measurement operation too much time-consuming to be acceptable.

In this work, we demonstrate a UAV-integrated sensing system capable of performing ultrasonic measurements of the depth of surface-opening cracks in concrete with sub-millimeter precision while flying. To the best of our knowledge, this is the first time that such measurement capabilities are demonstrated for an aerial vehicle. The system is based on the sensor positioning flexibility provided by the UAV technology presented in [20], an innovative aerial manipulator that allows the end-effector to slide on the contact surface while the vehicle is flying, and consequently to accurately place the ultrasonic transducers on the selected crack. This platform can maintain contact with the surface in a fully autonomous mode while a fine adjustment of the end-effector placement is performed by a remote operator. Crack depth and surface velocity ultrasound measurements performed by the UAV platform are demonstrated, using PZT transducers suitable for concrete driven by a lightweight custom electronic readout, which was purposely designed to fulfil the payload requirements of the aerial platform.

The system that we developed represents an advancement towards the automation of inspection and maintenance procedures on constructions, in which these measurements are generally performed manually. Performing ultrasonic measurements related to structural assessment of concrete structures by means of a UAV instead of sending operators to take manual measurements that are often needed on difficult to access areas on buildings and structures is particularly attractive for the possibility of avoiding risks for the operators and reducing the cost and time needed for the inspection.

2. System design and prototyping

The design of the ultrasound measurement system, of the UAV and the end effector, and the ultrasound measurement method adopted are described in the following.

2.1. Ultrasonic measurement method

Ultrasound measurements are largely employed in Non-Destructive Testing (NDT) of concrete structures for quality assessment of the material and for depth measurement of surface-opening cracks in it [21–23]. Such measurements are based on the method of ultrasound ToF estimation, which allows to determine the ultrasound velocity in concrete and has been standardized [24]. Based on it, a crack depth measurement can be realized in two phases, as illustrated in Fig. 1.

First (Fig. 1 top), a surface ultrasound velocity measurement on a concrete area without any crack opening is performed. In this measurement, an ultrasound emitter and a detector are placed in contact with concrete at a known distance a. Once generated by the emitter, the ultrasound wave propagates through concrete and reaches the detector after a propagation ToF t, depending on the velocity of sound in it. Since the shortest path between the transmitter and the detector is the one passing through the surface, the surface propagation velocity v of the ultrasound wave in concrete will be given by

$$v = \frac{a}{\tau} \tag{1}$$

After measuring the surface velocity, the transducers are placed at the two sides of a surface opening crack, as shown in Fig. 1 bottom. In this second measurement, the ultrasonic wave generated by the emitter cannot reach the detector by propagating through the surface, as in the first case. This happens because the crack acts as a barrier for the ultrasound waves, due to the acoustic impedance mismatch between concrete and air, and consequently the shortest acoustic path from the emitter to the detector is the one shown in the figure, in which the ultrasound wave reaches the deepest point of the crack and is scattered by its tip towards the surface.

In these conditions, the following equation holds involving the propagation time t, the crack depth h and the distance of the two transducers from the crack surface opening d:

$$h^2 = v^2\left(\frac{\tau}{2}\right)^2 - d^2 \tag{2}$$

Eq. (2) simply derives from the application of Pythagoras' theorem to the ultrasonic wave path depicted in Fig. 1 bottom, assuming that the two transducers are located at an equal distance d from the crack surface opening. Assuming a fixed distance a between the transducers, the identity $2d = a$ holds in Eqs. (1) and (2).

By first measuring the ultrasound speed v with the ToF measurement illustrated in Fig. 1 top and, afterwards, displacing the transducers across the crack as in Fig. 1 bottom, the depth of the crack h can be quite straightforwardly determined using Eq. (2).

The accuracy of the measurement depends upon the ability to precisely determine the distance between the transducers and on the precision of the ToF estimation. For the second problem, several methods have been presented in the literature to improve the ToF measurement accuracy and eliminate the need of a visual check of the acquired waveform, such as the fixed threshold [25], the zero-crossing [26], and the Akaike Information Criterion [27] algorithms. This is an aspect of

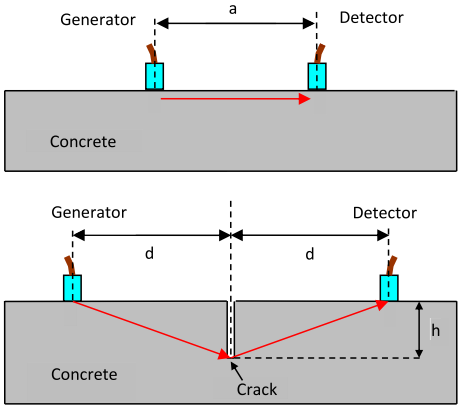

Fig. 1. Surface velocity (top) and crack depth (bottom) measurement performed by ultrasound ToF estimation.

paramount importance in autonomous inspections, both for speeding up the analysis, limiting the human interaction, and for reducing the subjectivity of the measurements when they are performed by different operators. In our system, we choose to implement the zero-crossing algorithm for automatic ToF estimation in the ultrasonic measurements.

Another important aspect in these measurements is the quality of the ultrasound coupling between the transducers and the surface of concrete. A suitable coupling material and sufficient applied pressure on the transducers must be used to obtain a clear ultrasonic signal for a reliable ToF estimation.

All these requirements can be in principle fulfilled by a measurement system integrated on a UAV that can perform contact operation with the following characteristics: automatic displacement of the transducers with pressure control, high voltage excitation and high signal to noise ratio detection for the ultrasonic transducers, as well as high resolution and accuracy in ToF estimation.

In the next section, the design of a system matching such specifications and suitable for use on a UAV will be described.

2.2. Ultrasonic measurement system

When examining commercially available ultrasound systems used for pulse velocity measurements, compact tools are readily available. However, these tools are generally unsuitable for conducting crack depth measurements in concrete. This limitation arises from the necessity for high actuation voltages on the piezoelectric transducers to generate the powerful waves required for ToF measurements in concrete. In contrast, small-sized readout circuits designed for ultrasonic transducers typically provide actuation voltages in the range of a few hundred volts, which would be inadequate for this specific application.

Following these considerations, a custom pulser/receiver unit was designed as illustrated in Fig. 2, where a 3D rendering image realized in software CAD Inventor® is shown. The readout was manufactured in a four-layers Printed Circuit Board (PCB) in FR4 material, with overall weigh of 90 g and size of 12 × 5 × 5 cm^3, including the package.

Thanks to its small size and weight, the custom unit can be easily integrated on the UAV and directly controlled by USB from the PC control unit of the vehicle to set the measurement parameters and acquire the results. The low power consumption allows the pulser/receiver unit to be powered by the main battery of the UAV, without significantly affecting the battery charge and consequently the maximum possible inspection time.

The readout circuit that was implemented in the ultrasound module was based on a high-resolution time to digital converter TDC7200 (from Texas Instruments), used to measure the ultrasonic ToF very accurately (55 ps time measurement resolution), and a TDC1000 ultrasonic sensing analogue front-end (also from Texas Instruments), employed to drive the piezoelectric transducer with a programmable voltage pulse and amplify the received signal. A PIC32MX microcontroller from Microchip Technology, equipped with USB communication, is used as an interface with the readout circuit and acquires the ultrasonic waveform that is subsequently transmitted to the aerial platform PC. Due to the large attenuation of acoustic waves in concrete, the piezoelectric transducer employed to generate the ultrasonic waves needs to be driven by a high voltage generator with sufficient output power and maximum voltage in the range of a few kV. In order to meet these requirements, a programmable high DC voltage generator in the range 0–100 V based on a LT3750 capacitor charger controller (from Linear technology), starting from a 5 V power supply, was included in the readout. The voltage pulse generated in this way was further amplified up to 3 kV by using a ZS1052 transformer (from Excelitas Technologies) with a 1:36 transformer ratio.

The PCB board block scheme and prototype picture are reported in Figs. 3 and 4, respectively.

Thanks to the flexibility of the designed system, transducers with different resonance frequencies and actuation voltages can be used, according to the characteristics of the materials under test. In concrete measurements, for example, high-voltage transducers operating at 54 kHz are usually employed, whereas, for measurements on steel, transducers with higher resonance frequency and significantly lower driving voltage are utilized, because the ultrasound attenuation is much lower in this case.

The pulser/receiver unit was preliminary tested before integration on the UAV with two 54 kHz transducers (from Pulsonic) by performing ToF and crack depth measurements on concrete specimens. In these experiments, the problem of acoustic impedance matching between the PZT transducers and the concrete specimen had to be addressed. Even though dry coupling (that is coupling without any interface material) on concrete is possible with specially designed transducers, the standard method makes use of an ultrasonic gel couplant. The function of this gel is to eliminate the air gap between the transducers and the surface of concrete and provide a sufficient acoustic impedance matching between the two materials to have a good ultrasound transmission between the transducers and concrete.

For the case of ultrasonic measurements from a UAV, the use of the coupling gel is evidently impractical, and consequently the adoption of non-liquid interface materials is mandatory. After several tests carried out with different elastomers and also with ultrasonic transducers designed for dry contact, we found out that the best results with our system could be obtained using plasticine as an ultrasound coupling material. Plasticine is a material commonly used for moulding, composed by clay, oil and wax, but it also has good ultrasonic transmission properties and is sometimes utilized to this purpose [28].

In the system, we applied a roughly 3 mm thick plasticine layer on the bottom face of the transducers to enhance the ultrasound coupling with the concrete surface. To eliminate the ultrasound delay taking place through the plasticine layers in the measurements, an initial calibration of the system was carried out by performing a ToF

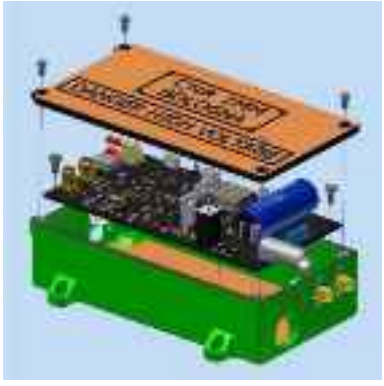

Fig. 2. 3D design of the custom ultrasound pulser/receiver unit employed in the crack depth and surface velocity measurements.

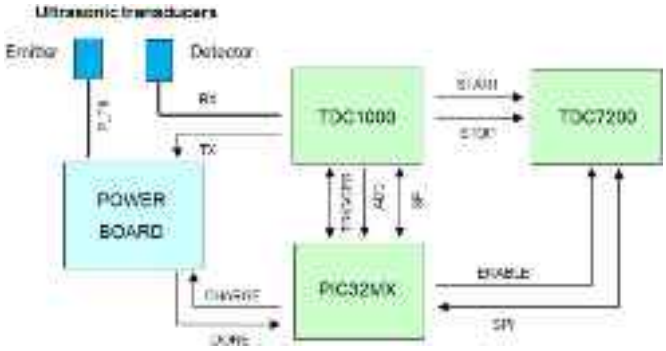

Fig. 3. Main block scheme of the custom ultrasound pulser/receiver unit.

Fig. 4. Custom pulser/receiver unit for ultrasonic measurements.

measurement on a metal specimen with a known ultrasound transit time, as illustrated in Fig. 5. This calibration step was used to estimate the ToF offset introduced by the plasticine layers, which was subsequently subtracted automatically from all the measurements performed in the tests carried out on concrete samples.

The calibration procedure relied on a purposely prepared sample (the black cylinder that is visible in Fig. 5 between the two ultrasonic transducers), which presents a known ultrasound transit time of 57.4 μsec. Such specimens are routinely employed in manual ultrasound measurements to calibrate the front-detection algorithm of commercial pulsers, using ultrasound gel couplants to interface the transducers to the specimen. In our case, we used plasticine as an interface layer, measuring a transit time that was larger than the expected 57.4 μsec because of the additional propagation delays introduced by plasticine. By calculating the difference between the measured ToF in the calibration procedure and the expected transit time of 57.4 μsec, the additional delay introduced by the plasticine interface layers was calculated. This delay was systematically subtracted in the measurements performed on concrete to eliminate the effect of the interface layers on the measured ToF.

After calibration, the system was tested on a homemade concrete specimen containing artificial cracks, applying a weight of 1.5 kg on each transducer during the measurement.

A typical result of the ToF laboratory measurements with a 2.5 kV peak voltage driving signal is reported in Fig. 6, where the oscilloscope trace of the ultrasonic signal acquired through the PZT receiver for a 5.9 cm deep crack is shown. This measurement yielded a calculated concrete ultrasound velocity of 4023 m/s and a measured depth of 5.94 cm.

Fig. 7 reports the results of 10 repeated ToF measurements performed in the same experimental conditions, showing a standard deviation lower than 0.005 μs. In the experiment, the transducers were positioned at 16 cm from each other with the crack in between. As can be seen from the test results reported in Fig. 7 the reproducibility of the measurement was very good. This was partly owing to the performances of the TDC1000 and TDC7200 components used in the readout and to the hardware-based zero-crossing detection algorithm implemented to calculate the ToF. In the TDC 1000 analog front end, after filtering and amplification of the received signal in the bandwidth of interest, the zero-crossing algorithm was implemented with a fast comparator that

Fig. 5. Ultrasonic measurement performed for the system calibration.

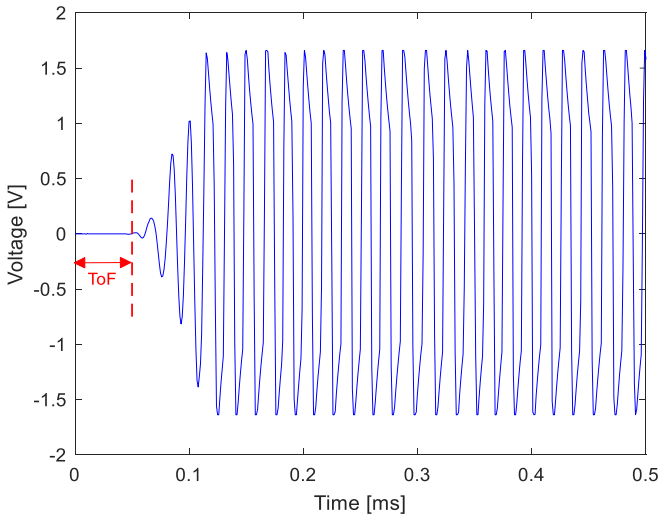

Fig. 6. Received ultrasound waveform acquired on a concrete specimen using the custom pulser/receiver unit with two 54 kHz transducers (5.9 cm deep crack).

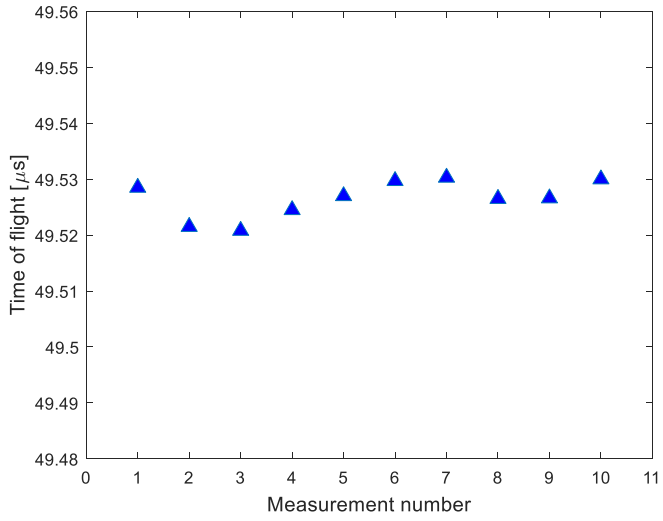

Fig. 7. Reproducibility of a set of repeated ToF measurements performed on a concrete specimen.

generated a square pulse when the acoustic signal crosses the zero level, which was then fed to the input of the TDC7200 for the ToF estimation.

Making use of plasticine as an interface layer, possible variations of the coupling layer thickness may potentially influence the accuracy of the measurement. However, during the laboratory tests it was observed that plasticine is relatively hard at room temperature and is not easily deformed during the ultrasonic measurements, even applying a force corresponding to 1.5 kg on the transducers. Consequently, frequent recalibration of the ToF offset with the method shown in Fig. 5 was not necessary in the experiments.

It is also worth noticing that, since the contact area between the piezoelectric transducer and the concrete sample is not negligible (the transmitter and the receiver have a circular shaped area with a diameter of 3 cm), a certain degree of uncertainty must be handled in the calculation of d and consequently in the derivation of v and h. In our experiments, the d value used in Eq. (2) was measured as the distance between the centres of the piezoelectric transducers; furthermore, the distance between the sensors was increased as much as possible to reduce the associated relative error. Such distance, however, cannot be increased too much because it affects the amplitude of the received acoustic wave

and, consequently, the measurement accuracy when the baseline noise becomes comparable to the signal level. Moreover, the size of the end-effector, which is related to the distance between the transducers, could not be increased too much for payload limitations. Consequently, a distance around 15 cm was chosen as an appropriate trade-off between these conflicting requirements, enabling a sufficient reduction of the error related to the size of the transducers and assuring, at the same time, a good amplitude of the detected wave, avoiding excessive attenuation, and an affordable size and weight of the end-effector.

2.3. UAV with robotic arm for contact measurements

The UAV system reported in Fig. 8 comprises three distinct components, the aerial platform, the robotic contact device, and the end effector.

The aerial platform is the main element: it hosts all the other components and has the responsibility of applying the required force to maintain good contact with the target surface during the ultrasonic measurements. This aerial robot is a multicopter with a diameter around 1.5 m and is able to carry a payload up to 2 kg at the end-effector. The robotic contact device is attached to the aerial platform by movable joints: it is a mechatronic device that allows the UAV to maintain a stationary contact of the end effector on the surface under test, thanks to its six degrees of freedom design. The main advantage of this configuration is that the aerial robot can keep stable contact of the end effector with the surface up to 50 km/h wind perturbations. To this purpose, the Inertial Measurement Unit (IMU) of the UAV is utilized to stabilize the vehicle in case of strong wind. However, it is true that under rapid changes of the perturbations the applied force can vary, and this issue must be resolved at sensor level. Moreover, to reduce perturbations like vibrations or contacted-force, different kind of dampeners are located in the mechatronic device and the end-effector. The end effector is installed on the tip of the robotic contact device and is equipped with wheels that are used to move it freely over the contact surface, while the UAV keeps flying. Its main task is to house the sensors that are needed to perform the required inspection on the surface, in this case the ultrasound transducers. The device also has a camera on its lower part that aids the operator in placing the transducers on the crack correctly. More details on the robotic arm, the end-effector design and the aerial platform can be found in [20].

3. Integration of the ultrasonic measurement system on the UAV and preliminary tests

The two 54 kHz high-power piezoelectric transducers utilized for the crack depth measurements were mounted on the UAV end effector at a distance of 15.4 cm from each other, as shown in Fig. 9. As mentioned before, such spacing was chosen after a careful evaluation of several factors, including the acoustic attenuation of ultrasound in concrete, the constraints related to the accuracy of the crack depth measurements, and the need to limit the size and weight of the end effector.

The integrated ultrasonic system was preliminary tested by contacting a concrete specimen containing two artificial cracks of different depths (respectively 3.5 and 5.4 cm) using the end-effector mounted on a still UAV kept on a support mimicking the possible position of the vehicle during the hovering measurements. These tests aimed at assessing the performance of the ultrasonic measurements operated from the end-effector without the disturbance of possible instabilities generated by the flying UAV.

Fig. 8. UAV with ultrasonic measurement system.

Fig. 9. Integration of the ultrasonic sensors on the end effector of the UAV.

During such experiments, the transducers were brought in contact with the concrete surface and the necessary pressure was applied on them using the end-effector displacement capabilities, with remote control.

In the measurements, two different placements of the PZT transducers were employed, following the measurement procedure formerly outlined in Section 2. Initially, the sensors were positioned beside the crack (as shown in Fig. 10). This configuration was utilized to conduct a straightforward ultrasound surface velocity measurement on the specimen. Subsequently, the sensors were repositioned across the crack (Fig. 11) to perform the depth measurements.

After positioning the end effector on the chosen location, the sensors were lowered using two independent stepper motors until they achieved an optimal contact with the specimen. Throughout all the testing procedure, the end effector spring was maintained in a compressed state, close to the maximum value expected to be possible during the airborne measurements. Such spring compression ensured to apply an adequate force on the sensors during the measurements.

To assess the reliability of the technique, several repeated measurements were conducted in these conditions. As shown in Tables 1 and 2, the method exhibited a good repeatability, evidenced by a standard deviation of less than 0.02 μs in repeated time-of-flight (ToF) measurements. For the 3.5 cm deep crack measurements, the average measured depth was 35.152 mm (average error margin 0.152 mm) with a standard deviation of 0.028 mm based on five measurements. For the 5.4 cm deep artificial crack, the average measured depth was 54.421 mm (average error margin 0.421 mm) with a standard deviation of 0.030 mm. The slightly larger deviation observed in these measurements compared to laboratory tests may be due to small variations in the

Fig. 10. End effector placement on specimen for surface velocity measurement.

Fig. 11. End effector placement on specimen for crack depth measurement.

Fig. 12. Airborne crack depth measurement performed on artificial specimen in a controlled flying environment.

Table 1
Repeatability test for the 3.5 cm deep crack measurements performed with the sensors integrated on the end effector from the steady UAV (measured ultrasonic speed: 2775 m/s).

Measurement Index (crack 1)	ToF (μs)	Estimated depth (mm)
1	61.011	35.156
2	60.998	35.112
3	61.008	35.146
4	61.012	35.159
5	61.021	35.189

Table 2
Repeatability test for the 5.4 cm deep crack measurements performed with the sensors integrated on the end effector from the steady UAV (measured ultrasonic speed: 2775 m/s).

Measurement Index (crack 2)	ToF (μs)	Estimated depth (mm)
1	67.984	54.473
2	67.962	54.420
3	67.958	54.410
4	67.954	54.401
5	67.954	54.401

pressure applied by the end effector to the transducers during the experiments.

The depth measurements of the cracks, determined through the ultrasound propagation velocity, exhibit relative errors of approximately 0.5 % and 0.8 % for cracks 1 and 2, respectively. These errors are quite comparable with those typically affecting traditional measurements performed manually using a liquid coupling gel. Such accuracy limitations can be attributed to several factors. First, a possible source of imprecision is the non-uniformity of the concrete itself. The ultrasonic speed measurement is, in fact, performed in the vicinity of the crack, rather than precisely on the crack location (which would not be possible in practice), introducing an error in the evaluation of the actual ultrasound velocity and consequently in the crack depth measurement. Moreover, other errors may come from the evaluation of the distance between the transducers, which is necessarily approximated because of the non-negligible size of the contact area of the transducers, as mentioned before. Other possible imprecisions can also be related, in theory, to small variations in the thickness of the plasticine used as an interface material on the transducers, but this error can be compensated by recalibrating the measurement offset, as explained earlier.

4. Airborne measurement tests

After completion of the static tests performed with the end effector tool, the system was tested in a controlled flying environment, as shown in Fig. 12. The sequence of operations executed in the tests was the following:

1. *Take-off and flight to the target.* The UAV took off and was remotely piloted up to the concrete specimen previously used in the static tests.
2. *Contact Initiation*: the end effector was positioned in hovering contact with the target surface through the extended arm and the spring system.
3. *Transition to Autonomous Mode*: once contact with the specimen was established, the operational mode of the UAV was switched from manual to autonomous control. In this autonomous mode, the system activated a closed-loop force control mechanism that ensured maintaining the end-effector in contact with the specimen with the UAV in hovering mode, always applying a constant pressure on the concrete surface.
4. *Adjustment of* the *end-effector position on the crack.* After setting the UAV in autonomous mode with the end-effector in contact with the specimen, the pilot adjusted the position of the sensors on the concrete surface by using the three motorized wheels of the end effector, aided by the camera that permitted a close view of the specimen. While the pilot performed this operation with a remote-control joystick, the autonomous closed-loop force control system kept the UAV in stable contact, maintaining the correct balance on the extended arm and following the movement of the end effector on the concrete surface. Using this procedure, the measurement tool could be correctly positioned on the specimen for the surface velocity and crack depth measurements, as explained before.
5. *Execution of the ultrasonic measurements.* Once the position of the end-effector was correct, the sensors were placed in contact with the surface using the stepper motors and the measurement was executed, while the UAV was still hovering in autonomous mode,
6. *Transition to remotely controlled mode, detachment, and landing of the UAV.* After completion of the ultrasonic measurements, the UAV was set in remotely controlled mode, was piloted away from the surface, and landed.

The ultrasonic signal acquired during these depth measurements for the 5.4 cm deep crack is reported in Fig. 13, resulting in a measured depth of 5.45 cm.

A closer inspection of the plot reveals that, even with the vibrations produced by the UAV during the airborne measurements, the rising edge of the waveforms remains clear, with no discernible noise affecting the signal baseline. The ToF estimation in the airborne measurement was the same measured in the static tests within a variation of 0.5 %, yielding an estimation of the crack depth of comparable accuracy.

The system was additionally tested during an on-field trial conducted as part of the European project RESIST (https://www.resistproject.eu/), which took place on the T9 Metsovo bridge in Greece in an outdoor environment and on a high-rise structure. In these tests, the ultrasonic measurements were executed at an elevation of approximately 35 m above ground, as shown in Fig. 14.

During these on-field tests, the previously outlined measurement procedure was followed to place the ultrasound tool on the bridge concrete surface and execute the measurements. The difference was the

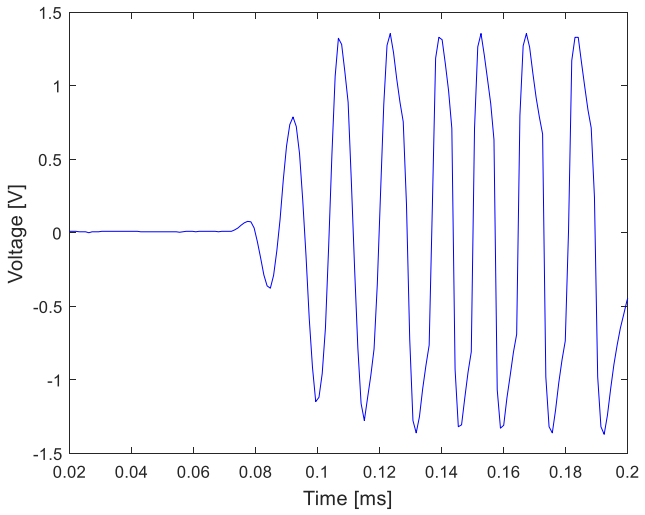

Fig. 13. Ultrasonic signal acquired during airborne crack depth measurement performed in a controlled flying environment (distance between the transducers adjusted to 16 cm in the airborne measurements).

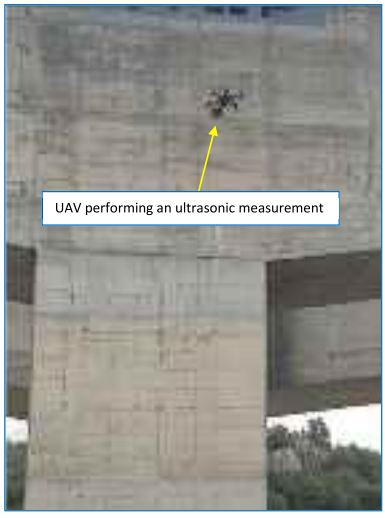

Fig. 14. Ultrasonic measurement performed on the T9 Metsovo bridge (Greece) by the UAV.

type of measurement performed: since no surface opening cracks were present in the structure, only surface velocity measurements were executed. Such measurement is also of interest for structural assessment, since the ultrasound velocity in concrete is related to the quality of the material, resulting in a decrease of the measured speed as the material degrades with age. Leveraging the degrees of freedom offered by the robotic arm, the UAV was able to reach any point of interest situated on the surfaces of the bridge beams and piles.

In Fig. 15, an example of ultrasonic signal acquired during the on-field measurements on the bridge is reported by way of example. The measurement shown in the figure yielded a ToF of 41.5 μs, which corresponds to a surface velocity of 3855 m/s.

To test the measurement repeatability of the system in on-field operating conditions, the same ultrasonic measurement was executed several times, as reported in Fig. 16. As can be seen from the different traces shown in the figure, corresponding to repeated airborne measurements, the reproducibility of the ToF estimation operated through the zero-crossing algorithm was very good, although some variations were observed in the acoustic wave intensity, which however are not relevant for the automatic ToF evaluation performed by the system.

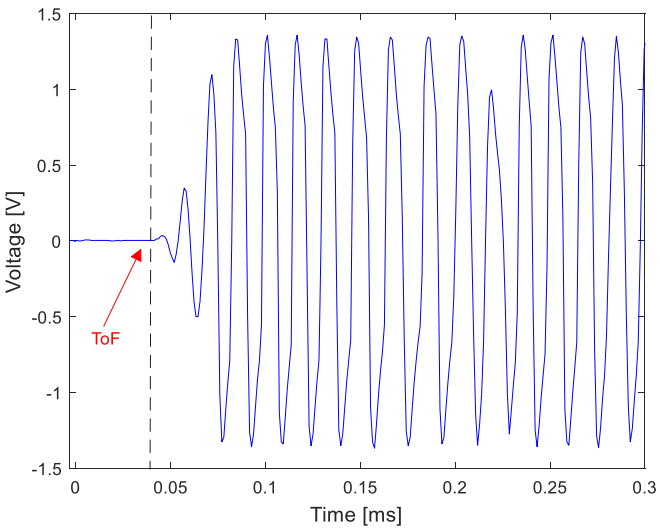

Fig. 15. Acoustic wave detected in the surface velocity measurement performed on the T9 Metsovo bridge (Greece).

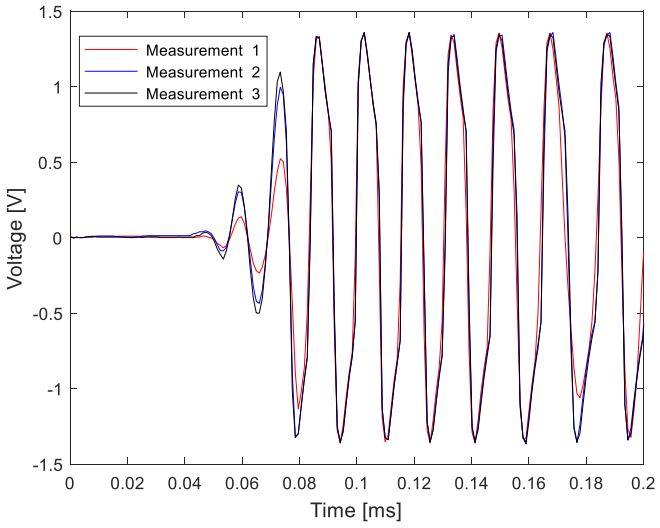

Fig. 16. Repeatability test in on-field airborne ultrasound measurement.

5. Discussion

In this section, a few issues related to the results presented above are discussed.

5.1. Comparison with other crack depth measurement methods on concrete

Crack depth measurement methods on concrete can be classified in two general categories: manual methods and automated methods. Generally speaking, automated methods are much less mature than manual methods, which are the standard in structural assessment practices nowadays, and are limited to some early examples recently reported as a result of research projects [6,23,29,30].

Considering manual methods, all of them share the same need of an expert operator that is expected to physically access the crack under measurement to evaluate the depth. This procedure includes two phases: first the cracks need to be visually identified on the concrete structure (this is normally carried out by locating the surface opening of the cracks on the external surface of the structure); afterwards, the located cracks are measured in selected positions with a method that is suitable to

determine their depth.

The simplest method that can be used to this purpose are crack depth cards [31]: these are flexible, thin rulers (their thickness is normally around 0.5 mm) that can be inserted into the surface opening of the cracks up to reaching the crack bottom, reading the depth on the graduated scale printed on the card. The main disadvantage of this method, which is, on the other hand, convenient for its simplicity and because it does not need the use of any electronic instrumentation, is the fact that in many cases using the card is not possible to reach the real bottom of the crack (this is particularly critical for deep and thin cracks and for cracks that present an irregular shape in the direction of the depth of the structure), and consequently the measured depth of the crack is often underestimated.

These limitations can be overcome with Non-Destructive measurement methods like ultrasound pulse propagation measurements. These measurements, whose principle has already been described in section 2.1, are the most often used for crack depth evaluation in concrete structures and custom portable ultrasonic pulsers have been developed for this purpose [32]. These tools are basically high-power portable electronic instruments that are suitable for operating a pair of piezoelectric ultrasound transducers to generate and detect an ultrasonic pulse across a surface opening crack and evaluate the ToF. In manual measurements, an expert operator is needed who, bringing the ultrasonic pulser and the transducers up to the location of the crack, operates the measurement. One of the critical aspects of this procedure is the ultrasonic coupling of the piezo transducers to the surface of concrete, which must be very good to obtain a reliable measurement. The standard method for that is the use of ultrasound gel couplants between the bottom surface of the transducers and the surface of concrete close to the crack under measurement. The gel acts as an acoustic impedance adaptor between the transducers and concrete, avoiding excessive attenuation of the generated wave when it propagates from the piezo actuator into concrete and, in detection mode, from concrete to the piezo sensor after propagation through the crack. The application of the gel couplant, which is relatively easy when performed manually, is one of the most complicated elements for automation of these measurement, because these gels are fluids, and this makes their integration within an automated procedure difficult.

With the automated method that we propose in this paper, we managed to overcome the problem of the gel couplants using plasticine, which is a solid material, instead of the fluids that are traditionally used in manual measurements.

An automated method presents evident advantages related to the safety and costs of the structure inspection when crack depth measurements are needed for that. In high-rise structures, such as bridges, the safety and cost issues are especially relevant, since for manual crack depth measurements the operator must be allowed to reach the location of the crack surface opening, which may be in difficult positions, requiring the use of scaffoldings or cranes. Moreover, the operation of accessing the location of the crack from a close distance may be needed twice: the first time to perform a mapping of the cracks on the structure (for high-rise constructions this may be impossible from the ground) and the second one to perform the contact measurements. Using a UAV as we propose in our method, the crack detection and depth measurements can be performed quite straightforwardly by two flight missions: the first one using cameras to locate the cracks on the structure, the second one to measure crack depth in selected positions with the special end-effector that we have developed. Since in this case no scaffolding or cranes are needed, the reduction of cost and time required is significant compared to the case of manual measurements, considering that with the UAV-based technique several crack depth measurements would be possible in one flight mission (each measurements requires few minutes, most of the time being needed to approach the crack with the UAV and place the end-effector in the correct positions for the measurements).

5.2. Influence of environmental factors on the measurements

The UAV-based measurement method proposed in this paper can be affected by environmental factors for two main reasons. The first reason depends on the fact that, to perform the measurements, the UAV must be able to fly around the structure of interest. This condition makes the automated measurements undergo all the environmental limitations that the flight of UAVs present, such as absence of heavy rain and too strong wind. The second reason can be related to the influence of the environmental conditions on the automated ultrasonic measurement, independently from the flight-enabling related environmental factors. In this respect, it is worth noticing that the ToF ultrasonic measurements needed for crack depth estimation do not present a marked dependency on environmental conditions like temperature and relative humidity of air. Using contact ultrasound propagation and detection as in the method proposed, the propagation of ultrasonic waves in air is not important in the measurements and the main parameter affecting the propagation velocity in concrete during the crack depth measurements is the Elastic Modulus of concrete. This parameter shows a weak dependence on ambient temperature, but this does not affect significantly the crack depth measurements because of the reference propagation velocity measurement that is performed before the actual crack depth ToF (please refer to section 2.1). Also, relative humidity of air is not very important because the waves do not propagate through air during the measurements, as long as the crack space or the surface of concrete is not completely wet (again this may be a problem only in the presence of heavy rain, which however would make the flight mission of the UAV impossible). Considering the effect of temperature, the specific issues related to the use of plasticine as a coupling layer that we have proposed deserve a mention. Plasticine is a solid material whose stiffness is quite dependent on temperature, being softer at higher temperatures and harder at lower temperatures. Since the rigidity of the material influences the ultrasound propagation velocity in it, and compensating the ultrasound propagation delays in plasticine is essential to obtain accurate measurements, the calibration procedure described in Section 2.2 must be repeated if the ambient temperature varies too much from one measurement mission to another, because the ToF of the ultrasound waves within the plasticine layers would not be the same in the two cases.

5.3. Accuracy limitations of the measurements, possible sources of error and compensation techniques

Besides the well-known accuracy limitations of the ToF-based ultrasonic measurements already discussed earlier in this paper (such as the limitations in the accuracy of the pulse front detection and the issues related to the possible inhomogeneity of the concrete close to the crack), some specific sources of error more closely related to the automated UAV-based measurements that we have developed can be discussed. As already mentioned in Section 2.2, the use of the plasticine layer as a coupling material between the piezo transducers and the surface of concrete is an essential part of the automated measurements. Since the ultrasonic delay within the plasticine layers is not negligible in the calculation of the ToF, it must be subtracted by the raw measurement not to affect the accuracy of the surface velocity and crack depth measurements performed by the UAV. These delays depend on the thicknesses of the plasticine layers applied on the transducers and on the elastic modulus of the material. At room temperature, plasticine is relatively hard but however it is plastic and after pressing the transducers on concrete for several times, some small thickness variation is possible. Consequently, the calibration procedure illustrated in Section 2.2, which serves as a compensation of the ultrasonic delays in the plasticine interface layers, should be repeated regularly during a measurement campaign to check for any changes in the calibration parameters and to adjust the compensation.

Another possible source of error in the automated measurements

may come from placement inaccuracies of the end-effector on the crack, because of which the distances of the two transducers from the crack surface opening may not be the same. The situation in this case would be the one represented in Fig. 17, in which, for instance, the distance of the ultrasound generator from the crack (d_1) happens to be lower than the one of the detector (d_2).

In this case, it is easy to verify that the following formula could be used to calculate the depth of the crack instead of eq. (2) reported before.

$$\tau = \frac{1}{v}\left(\sqrt{d_1^2 + h^2} + \sqrt{d_2^2 + h^2}\right) \tag{3}$$

Eq. (3) is a nonlinear equation that can be solved graphically or numerically for h once the overall ultrasound propagation velocity v and the ToF τ are determined from the ultrasonic measurements and the distances d_1, d_2 are independently measured. To this purpose, the camera mounted on the end effector can be usefully employed since an arrow marker was placed on it in the middle of the distance between the two transducers. By simply taking a picture with the camera after placing the end effector on the crack, the distances d_1, d_2 can be straightforwardly determined by measuring the distance of the marker from the crack on the image. This is possible because, due to the design of the end-effector, the camera is placed at a fixed focus distance from the surface under measurement during contact, and consequently a direct correlation between the distance in pixels between two points in the image captured by the camera on the surface and the actual distance in millimetres between these two points on the surface itself can be established.

5.4. Cost, regulation and integration issues related to the UAV measurements

The aerial platform that we used for the measurements has a manufacturing cost of about 25,000 euros with an estimated cost for annual maintenance of 5000 euros, based on 200 h of flight per year. To these costs, the salary of the UAV pilot should be added to estimate the hourly cost of the inspection including the crack measurements. However, no cranes or scaffolding would be necessary to reach the measurement sites, and this would allow for saving costs and greatly reducing the time needed for the inspection. Regarding regulation related to the use of UAVs, different rules exist depending on the country. In Europe, a clear regulation has been approved for UAVs that establishes the needed safety rules and permits an experienced operator to use UAVs for civil purposes. The proposed method could also be relatively smoothly integrated into existing inspection workflows in which, typically, a visual inspection is performed as a first step to locate defects and visible cracks on the structure. After locating and mapping the cracks with this visual inspection, the UAV could be sent to measure the main cracks on the structure to evaluate their depth. Exploiting recent developments in computer vision techniques performed by UAVs, the same aerial platform could be possibly used first to locate the cracks using medium-distance cameras and, afterwards, to perform the crack measurements with the method described in this paper.

6. Conclusions

The UAV system described in this paper proved to be usable to perform accurate airborne ultrasonic crack depth and surface velocity measurements on concrete structures. The results presented confirmed the possibility to automate these measurements using a UAV instead of performing them manually, as is normally done in construction maintenance practice. Considering the risks and costs associated with the need to reach the inspection sites, particularly in high-rise buildings, the importance of automating the ultrasound measurements needed for structural assessment of constructions by means of an aerial vehicle

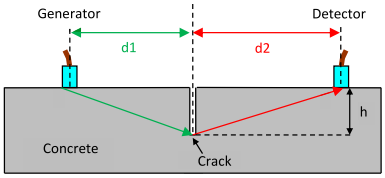

Fig. 17. Crack depth measurement by ultrasound ToF estimation with alignment error of the transducers on the crack.

appears clear. The use of a semi-autonomous vehicle like the one presented here is especially convenient for the purpose, because it enables maintaining contact with the concrete surface in a fully automatic way during the measurement and the only task required for the remote pilot is placing the robotic arm on the desired measurement point, such as a crack. After positioning the arm, the ultrasound measurement can be performed in a completely automatic way in a few seconds while the UAV keeps flying, without the need for any landing procedure. These capabilities enable the execution of several measurements during the same flight mission of the UAV, greatly reducing the time needed for the inspection procedures. Moreover, the placement accuracy of the system on a concrete wall is sufficient to cope with the demanding requirements of the crack depth measurement performed by ultrasonic ToF estimation (placement accuracy of few mm). The use of a plasticine layer demonstrated to be an effective dry contact method between the ultrasonic transducers and concrete, providing the possibility to perform accurate ToF measurements with a precision that was comparable to the one obtained with the manual method based on the ultrasound coupling gel, but in a much more effective way for use on a UAV. Possible variations of thickness of the plasticine layer taking place during the measurements could be handled with a periodic recalibration of the ToF offset using a standard calibration specimen. Exploiting the progress recently obtained in automatic crack detection by computer vision techniques [33–35] and with the improvement of the navigation capabilities of UAVs [36–38], the method presented here could be potentially used in the future for fully autonomous crack detection and measurement, and for automatic concrete quality evaluation by surface velocity measurements on concrete buildings and structures.

CRediT authorship contribution statement

Luca Belsito: Writing – original draft, Validation, Supervision, Software, Methodology, Investigation, Funding acquisition, Formal analysis, Data curation, Conceptualization. **Diego Marini:** Writing – original draft, Methodology. **Luca Masini:** Software, Methodology. **Matteo Ferri:** Writing – original draft, Validation, Methodology. **Miguel Ángel Trujillo:** Validation, Supervision, Software, Project administration, Methodology. **Antidio Viguria:** Validation, Supervision. **Alberto Roncaglia:** Writing – original draft, Validation, Supervision, Methodology, Investigation.

Declaration of competing interest

The authors declare the following financial interests/personal relationships which may be considered as potential competing interests:

Luca Belsito reports financial support was provided by European Commission. If there are other authors, they declare that they have no known competing financial interests or personal relationships that could have appeared to influence the work reported in this paper.

Acknowledgments

This work has received funding from the European Union's Horizon 2020 research and innovation programme under grant agreement No. 687384 and No. 769066. The contribution of Mr. Federico Zardi in the

PCB manufacturing and in the on-field tests is acknowledged.

Data availability

Data will be made available on request.

References

[1] State of infrastructure maintenance, European Commission Discussion paper. https://ec.europa.eu/docsroom/documents/34561.

[2] K. Gkoumas, M. van Balen, M. Grosso, F. Pekár, F.L. Marques Dos Santos, G. Haq, A. Ortega Hortelano, A. Tsakalidis, "Research and Innovation in Bridge Maintenance, Inspection and Monitoring – A European Perspective Based on the Transport Research and Innovation Monitoring and Information System (TRIMIS)", Publications Office, European Commission: Joint Research Centre, 2019, https://doi.org/10.2760/16174.

[3] R.J. Woodward, D.W. Cullington, A.F. Daly, P.R. Vassie, P. Haardt, R. Kashner, R. Astudillo, C. Velando, M.B. Godart, M.C. Cremona, B. Mahut, A. Raharinaivo, D. Lau, I. Markey, L. Bevc, I. Peruš, BRIME Project Final report. https://trimis.ec.europa.eu/project/bridge-management-europe#tab-docs.

[4] S. Yehia, O. Abudayyeh, I. Fazal, D. Randolph, A decision support system for concrete bridge deck maintenance, Adv. Eng. Softw. 39 (3) (2008) 202–210, https://doi.org/10.1016/j.advengsoft.2007.02.002.

[5] E. Ciampa, L. De Vito, M.R. Pecce, Practical issues on the use of drones for construction inspections, J. Phys. Conf. Ser. 1249 (1) (2019), https://doi.org/10.1088/1742-6596/1249/1/012016 art. no. 012016.

[6] K. Loupos, A.D. Doulamis, C. Stentoumis, E. Protopapadakis, K. Makantasis, N. D. Doulamis, A. Amditis, P. Chrobocinski, J. Victores, R. Montero, E. Menendez, C. Balaguer, R. Lopez, M. Cantero, R. Navarro, A. Roncaglia, L. Belsito, S. Camarinopoulos, N. Komodakis, P. Singh, Autonomous robotic system for tunnel structural inspection and assessment, Int. J. Intell. Robot. Appl. 2 (1) (2018) 43–66, https://doi.org/10.1007/s41315-017-0031-9.

[7] Y. Bao, Z. Tang, H. Li, Y. Zhang, Computer vision and deep learning–based data anomaly detection method for structural health monitoring, Struct. Health Monit. 18 (2) (2019) 401–421, https://doi.org/10.1177/1475921718757405.

[8] H. Nguyen, N.-D. Hoang, Computer vision-based classification of concrete spall severity using metaheuristic-optimized extreme gradient boosting machine and deep convolutional neural network, Autom. Constr. 140 (2022), https://doi.org/10.1016/j.autcon.2022.104371 art. no. 104371.

[9] I.-H. Kim, H. Jeon, S.-C. Baek, W.-H. Hong, H.-J. Jung, Application of crack identification techniques for an aging concrete bridge inspection using an unmanned aerial vehicle, Sensors 18 (6) (2018), https://doi.org/10.3390/s18061881 art. no. 1881.

[10] H. Su, X. Wang, T. Han, Z. Wang, Z. Zhao, P. Zhang, Research on a U-net bridge crack identification and feature-calculation methods based on a CBAM attention mechanism, Buildings 12 (10) (2022), https://doi.org/10.3390/buildings12101561 art. no. 1561.

[11] H. Yu, W. Yang, H. Zhang, W. He, A UAV-based crack inspection system for concrete bridge monitoring, in: International Geoscience and Remote Sensing Symposium (IGARSS), 2017-July, 2017, pp. 3305–3308, https://doi.org/10.1109/IGARSS.2017.8127704, art. no. 8127704.

[12] R. Caballero, J. Parra, M.Á. Trujillo, F.J. Pérez-Grau, A. Viguria, A. Ollero, Aerial robotic solution for detailed inspection of viaducts, Appl. Sci. (Switzerland) 11 (18) (2021), https://doi.org/10.3390/app11188404 art. no. 8404.

[13] G. Heredia, A.E. Jimenez-Cano, I. Sanchez, D. Llorente, V. Vega, J. Braga, J. A. Acosta, A. Ollero, Control of a multirotor outdoor aerial manipulator, in: IEEE International Conference on Intelligent Robots and Systems, 2014, pp. 3417–3422, https://doi.org/10.1109/IROS.2014.6943038, art. no. 6943038.

[14] P.J. Sanchez-Cuevas, P. Ramon-Soria, B. Arrue, A. Ollero, G. Heredia, Robotic system for inspection by contact of bridge beams using UAVs, Sensors (Switzerland) 19 (2) (2019), https://doi.org/10.3390/s19020305 art. no. 305.

[15] R. Watson, M. Kamel, D. Zhang, G. Dobie, C. Macleod, S.G. Pierce, J. Nieto, Dry coupled ultrasonic non-destructive evaluation using an over-actuated unmanned aerial vehicle, IEEE Trans. Autom. Sci. Eng. 19 (4) (2022) 2874–2889, https://doi.org/10.1109/TASE.2021.3094966.

[16] D. Zhang, R. Watson, C. MacLeod, G. Dobie, W. Galbraith, G. Pierce, Implementation and evaluation of an autonomous airborne ultrasound inspection system, Nondestruct. Test. Eval. 37 (1) (2022) 1–21, https://doi.org/10.1080/10589759.2021.1889546.

[17] R. Dahlstrom, Aerial robots for contact-based ultrasonic thickness measurements for field inspections, Mater. Eval. 79 (7) (2021) 687–694, https://doi.org/10.32548/2021.me-04213.

[18] P.A. Doyle, C.M. Scala, Crack depth measurement by ultrasonics: a review, Ultrasonics 16 (4) (1978) 164–170, https://doi.org/10.1016/0041-624X(78)90072-0.

[19] D. Marini, L. Belsito, L. Masini, M.A. Trujillo, A.L. Petrus, D. Martinez, F. Gamero, J.M. Barrientos, E. Blanco, A. Roncaglia, Acoustic micro-opto-mechanical transducers for crack width measurement on concrete structures from aerial robots, in: 20th International Conference on Solid-State Sensors, Actuators and Microsystems and Eurosensors XXXIII, TRANSDUCERS 2019 and EUROSENSORS XXXIII, 2019, pp. 893–896, https://doi.org/10.1109/TRANSDUCERS.2019.8808296, art. no. 8808296.

[20] M.Á. Trujillo, J.R. Martínez-De Dios, C. Martín, A. Viguria, A. Ollero, Novel aerial manipulator for accurate and robust industrial NDT contact inspection: a new tool for the oil and gas inspection industry, Sensors (Switzerland) 19 (6) (2019), https://doi.org/10.3390/s19061305 art. no. 1305.

[21] G. Karaiskos, A. Deraemaeker, D.G. Aggelis, D. Van Hemelrijck, Monitoring of concrete structures using the ultrasonic pulse velocity method, Smart Mater. Struct. 24 (11) (2015), https://doi.org/10.1088/0964-1726/24/11/113001 art. no. 113001.

[22] M. Seher, C.-W. In, J.-Y. Kim, K.E. Kurtis, L.J. Jacobs, Numerical and experimental study of crack depth measurement in concrete using diffuse ultrasound, J. Nondestruct. Eval. 32 (1) (2013) 81–92, https://doi.org/10.1088/0964-1726/24/11/113001.

[23] L. Belsito, L. Masini, M. Sanmartin, K. Loupos, A. Roncaglia, Ultrasonic sensor system for automatic depth measurement of surface opening cracks in concrete by means of a robotic arm, in: Transforming the Future of Infrastructure through Smarter Information - Proceedings of the International Conference on Smart Infrastructure and Construction, ICSIC 2016, 2016, pp. 239–244, https://doi.org/10.1680/tfitsi.61279.239.

[24] "Standard Test Method for Pulse Velocity through Concrete", ASTM Standard C597–16. https://www.astm.org.

[25] G. Andria, F. Attivissimo, N. Giaquinto, Digital signal processing techniques for accurate ultrasonic sensor measurement, Measurement 30 (2) (2001) 105–114, https://doi.org/10.1016/S0263-2241(00)00059-2.

[26] L. Svilainis, Review of high resolution time of flight estimation techniques for ultrasonic signals, in: 52nd Annual Conference of the British Institute of Non-Destructive Testing 2013, NDT 2013, 2013, pp. 231–242.

[27] H. Akaike, A new look at the statistical model identification, IEEE Trans. Autom. Control 19 (6) (1974) 716–723, https://doi.org/10.1109/TAC.1974.1100705.

[28] A. Carreon, A. Baltazar, J.-Y. Kim, Determination of contact evolution on a soft hemispherical probe using ultrasound, IEEE Sensors J. 15 (9) (2015) 5303–5311, https://doi.org/10.1109/JSEN.2015.2439293, art. no. 7118647.

[29] S. Dubey, B. Kumar, S. Ray, Heterogeneity induced fracture characterization of concrete under fatigue loading using digital image correlation and acoustic emission techniques, Int. J. Fatigue 188 (2024), https://doi.org/10.1016/j.ijfatigue.2024.108474 art. no. 108474.

[30] W. Li, J. Zhu, K. Mu, W. Yang, X. Zhang, X. Zhao, Experimental investigation of concrete crack depth detection using a novel piezoelectric transducer and improved AIC algorithm, Buildings 14 (12) (2024), https://doi.org/10.3390/buildings14123939 art. no. 3939.

[31] SV-artikel Germany, Crack Depth (n.d.), accessed 19 May 2025, https://sv-artikel.de/en/crack-inspection/crack-depth/.

[32] Controls, PULSONIC Ultrasonic Pulse Analyzer (n.d.), accessed 19 May 2025, https://controls-group.com/product/ultrasonic-pulse-analyzer/.

[33] L.M. Dang, H. Wang, Y. Li, Y. Park, C. Oh, T.N. Nguyen, H. Moon, Automatic tunnel lining crack evaluation and measurement using deep learning, Tunn. Undergr. Space Technol. 124 (2022), https://doi.org/10.1016/j.tust.2022.104472 art. no. 104472.

[34] Q. Mei, M. Gül, M.R. Azim, Densely connected deep neural network considering connectivity of pixels for automatic crack detection, Autom. Constr. 110 (2020), https://doi.org/10.1016/j.autcon.2019.103018 art. no. 103018.

[35] E. Protopapadakis, A. Voulodimos, A. Doulamis, N. Doulamis, T. Stathaki, Automatic crack detection for tunnel inspection using deep learning and heuristic image post-processing, Appl. Intell. 49 (7) (2019) 2793–2806, https://doi.org/10.1007/s10489-018-01396-y.

[36] P. Carrasco, F. Cuesta, R. Caballero, F.J. Perez-Grau, A. Viguria, Monte-Carlo localization for aerial robots using 3D LiDAR and UWB sensing, in: 2021 International Conference on Unmanned Aircraft Systems, ICUAS 2021, 2021, pp. 354–360, https://doi.org/10.1109/ICUAS51884.2021.9476732, art. no. 9476732.

[37] Minh D. Tuyet, Dung N. Ba, Hybrid algorithms in path planning for autonomous navigation of unmanned aerial vehicle: a comprehensive review, Meas. Sci. Technol. 35 (11) (2024), https://doi.org/10.1088/1361-6501/ad66f5 art. no. 112002.

[38] G. Haile, J. Lim, UAV-BS operation plan using reinforcement learning for unified communication and positioning in GPS-denied environment, IEICE Trans. Commun. E107.B (10) (2024) 681–690, https://doi.org/10.23919/transcom.2023EBP3174.